

# LOW MASS NEW PHYSICS SEARCH FOR A CP-ODD HIGGS BOSON $A^0$ DECAYING TO $s\bar{s}$ OR GLUON GLUON AT *BABAR*

E. GUIDO

on behalf of the *BABAR* Collaboration

*Università degli Studi di Genova, Department of Physics, Via Dodecaneso 33, I-16146 Genova, Italy*

We report on the search for the decay  $\Upsilon(1S) \rightarrow \gamma A^0$ ,  $A^0 \rightarrow gg$  or  $s\bar{s}$ , where  $A^0$  is the pseudoscalar light Higgs boson predicted by the next-to-minimal supersymmetric standard model. A sample of  $\sim 18 \times 10^6$   $\Upsilon(1S)$  resonances, produced in the *BABAR* experiment via  $e^+e^- \rightarrow \Upsilon(2S) \rightarrow \pi^+\pi^-\Upsilon(1S)$ , is used for this search. No significant signal has been found, and upper limits at the 90% of confidence level are set on the product branching fraction of the process.

## 1 Introduction

The Next to Minimal Supersymmetric Standard Model (NMSSM)<sup>1</sup>, one of the several extensions of the Standard Model, predicts a larger Higgs sector, with two charged, three neutral CP-even, and two neutral CP-odd Higgs bosons. In particular, the model includes the possibility that one of the pseudoscalar Higgs bosons, denoted as  $A^0$  hereafter, can be lighter than two bottom quarks<sup>2</sup>, therefore making its production accessible at the B-factories, via the radiative decay of an  $\Upsilon$  resonance.

The  $A^0$  is a superposition of a singlet and a non-singlet state, and the value of the branching fraction of the radiative decay  $\Upsilon \rightarrow \gamma A^0$  actually depends on the non-singlet fraction. The final state to which the  $A^0$  decays depends instead on various parameters, such as  $\tan\beta$  and the mass of the CP-odd Higgs boson itself<sup>3</sup>. In order to be sensitive to as much parameter space as possible, *BABAR* has performed searches for different final states:  $A^0$  decaying into  $\mu^+\mu^-$ <sup>4,5</sup>, into  $\tau^+\tau^-$ <sup>6,7</sup>, into invisible states<sup>8</sup>, and into hadrons<sup>9</sup>, without seeing any significant signal.

The search presented here<sup>10</sup> focuses on the decays  $A^0 \rightarrow gg$  or  $s\bar{s}$ . For an  $A^0$  mass smaller than  $2m_\tau$ , the light pseudoscalar Higgs boson is predicted to decay mostly into two gluons if  $\tan\beta$  is of order 1, and into  $s\bar{s}$  if  $\tan\beta$  is of order 10. Despite being motivated by NMSSM, the results of this search can be applied to any CP-odd hadronic resonances produced in the radiative decays of  $\Upsilon(1S)$ .

## 2 Experimental technique

This analysis uses the data recorded by the *BABAR* detector at the PEP-II asymmetric-energy  $e^+e^-$  collider at the SLAC National Accelerator Laboratory. The *BABAR* detector is described in detail elsewhere<sup>11,12</sup>. We use  $\sim 14 \text{ fb}^{-1}$  of data taken at the  $\Upsilon(2S)$  resonance. Tagging the dipion in the  $\Upsilon(2S) \rightarrow \pi^+\pi^-\Upsilon(1S)$  transition allows to significantly reduce the otherwise dominant  $e^+e^- \rightarrow q\bar{q}$  background, where  $q$  is a  $u$ ,  $d$ , or  $s$  quark. We also use  $\sim 1.4 \text{ fb}^{-1}$  of data taken 30 MeV below the  $\Upsilon(2S)$  resonance as a background estimate. Simulated signal events with various  $A^0$  masses ranging from 0.5 to 9.0 GeV/ $c^2$  are used in this analysis.

Table 1: Decay modes for candidate  $A^0 \rightarrow gg$  and  $s\bar{s}$  decays, sorted by the total mass of the decay products.

#	Channel	#	Channel
1	$\pi^+\pi^-\pi^0$	14	$K^+K^-\pi^+\pi^-$
2	$\pi^+\pi^-2\pi^0$	15	$K^+K^-\pi^+\pi^-\pi^0$
3	$2\pi^+2\pi^-$	16	$K^\pm K_S^0 \pi^\mp \pi^+ \pi^-$
4	$2\pi^+2\pi^-\pi^0$	17	$K^+K^-\eta$
5	$\pi^+\pi^-\eta$	18	$K^+K^-2\pi^+2\pi^-$
6	$2\pi^+2\pi^-2\pi^0$	19	$K^\pm K_S^0 \pi^\mp \pi^+ \pi^- 2\pi^0$
7	$3\pi^+3\pi^-$	20	$K^+K^-2\pi^+2\pi^-\pi^0$
8	$2\pi^+2\pi^-\eta$	21	$K^+K^-2\pi^+2\pi^-2\pi^0$
9	$3\pi^+3\pi^-2\pi^0$	22	$K^\pm K_S^0 \pi^\mp 2\pi^+2\pi^-\pi^0$
10	$4\pi^+4\pi^-$	23	$K^+K^-3\pi^+3\pi^-$
11	$K^+K^-\pi^0$	24	$2K^+2K^-$
12	$K^\pm K_S^0 \pi^\mp$	25	$p\bar{p}\pi^0$
13	$K^+K^-2\pi^0$	26	$p\bar{p}\pi^+\pi^-$

The final states analyzed must contain: two charged tracks as the dipion system candidate, a radiative photon with an energy greater than 200 MeV when calculated in its center-of-mass frame, and a hadronic system. An exclusive reconstruction of  $A^0 \rightarrow gg$  is performed, using 26 channels as listed in Table 1, while disregarding two-body decay channels because a CP-odd Higgs boson cannot decay into two pseudoscalar mesons. The  $A^0 \rightarrow s\bar{s}$  sample is defined as the subset of the 26  $A^0 \rightarrow gg$  decay channels that include two or four kaons (channels 11-24 in Table 1). Charged kaons, pions, and protons are required to be positively identified.

The  $A^0$  mass resolution is improved by constraining the  $A^0$  candidate and the photon to have an invariant mass equal to the  $\Upsilon(1S)$  one, and a decay vertex at the beam spot. The main backgrounds to this search are:

- $\Upsilon(1S) \rightarrow \gamma gg$  events, with gluons hadronizing to more than one daughter; it is dominant at low masses, *i.e.* between 2 and 4 GeV/c<sup>2</sup>;
- $\Upsilon(1S) \rightarrow ggg$  events, with a  $\pi^0$  mistaken as a photon; it is dominant at higher masses, *i.e.* between 7 and 9 GeV/c<sup>2</sup>.

This search relies on the hadronization modelling used in simulations; the agreement between data and Monte Carlo samples is checked on  $\Upsilon(1S) \rightarrow \gamma gg$  events, resulting in a scaling factor and a global systematic uncertainty of 50% to be applied to the efficiency. This is the dominant contribution to the systematic uncertainties of this analysis.

### 3 Results

The candidate mass spectrum is shown in Fig. 1. The  $A^0$  would appear as a narrow peak in the distribution. A scan of the mass spectrum has been performed in 10 MeV/c<sup>2</sup>-steps, from 0.5 to 9 GeV/c<sup>2</sup>, without finding any significant signal through the entire mass range analyzed. Bayesian upper limits at the 90% of confidence level are then set on the product of branching fractions  $\mathcal{B}(\Upsilon(1S) \rightarrow \gamma A^0) \times \mathcal{B}(A^0 \rightarrow gg)$  and  $\mathcal{B}(\Upsilon(1S) \rightarrow \gamma A^0) \times \mathcal{B}(A^0 \rightarrow s\bar{s})$ , ranging between 10<sup>-6</sup> and 10<sup>-2</sup>, and between 10<sup>-5</sup> and 10<sup>-3</sup> for the two final states, respectively, as shown in Fig. 2. As a result, the low mass region for  $A^0$  is excluded, and no evidence either for a light pseudoscalar Higgs boson, or for any narrow hadronic resonance is found through the entire mass spectrum.

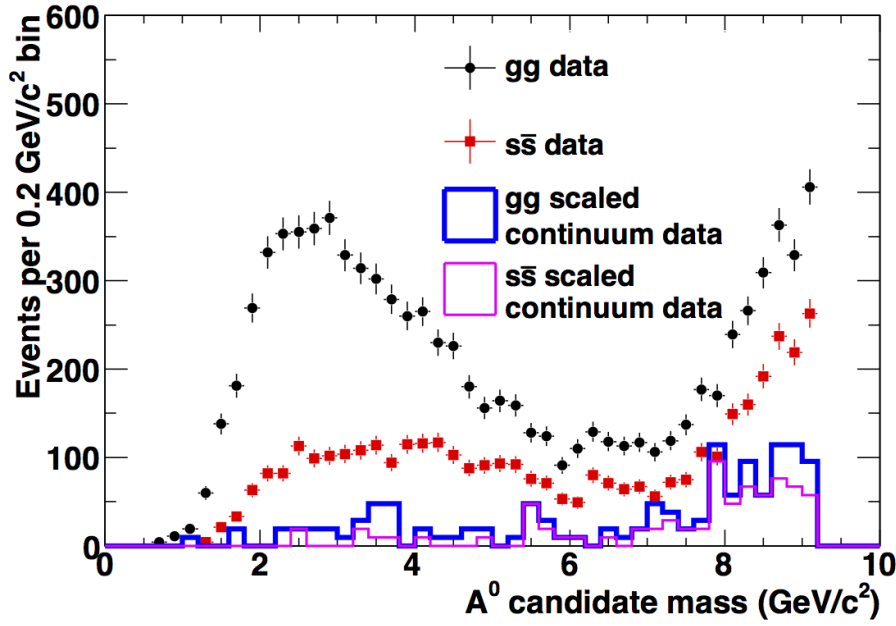


Figure 1:  $A^0$  candidate mass spectra after applying all selection criteria. We reconstruct  $A^0 \rightarrow gg$  using the 26 channels listed in Table 1 and  $A^0 \rightarrow s\bar{s}$  using the subset of the same 26 channels that includes two or four kaons. The  $A^0$  candidate mass is the invariant mass of the reconstructed hadrons in each channel. The black points with error bars are on-resonance data for  $A^0 \rightarrow gg$ . The red squares with error bars are on-resonance data for  $A^0 \rightarrow s\bar{s}$ . The thick blue histogram is  $A^0 \rightarrow gg$  in off-resonance data normalized to the on-resonance integrated luminosity. The thin magenta histogram is  $A^0 \rightarrow s\bar{s}$  in off-resonance data normalized to the on-resonance integrated luminosity.

## References

1. M. Maniatis, Int. J. Mod. Phys. A **25** (2010) 3505 [arXiv:0906.0777 [hep-ph]].
2. R. Dermisek, J. F. Gunion and B. McElrath, Phys. Rev. D **76** (2007) 051105 [hep-ph/0612031].
3. R. Dermisek and J. F. Gunion, Phys. Rev. D **81** (2010) 075003 [arXiv:1002.1971 [hep-ph]].
4. B. Aubert *et al.* [BaBar Collaboration], Phys. Rev. Lett. **103** (2009) 081803 [arXiv:0905.4539 [hep-ex]].
5. J. P. Lees *et al.* [BaBar Collaboration], Phys. Rev. D **87** (2013) 3, 031102 [arXiv:1210.0287 [hep-ex]].
6. B. Aubert *et al.* [BaBar Collaboration], Phys. Rev. Lett. **103** (2009) 181801 [arXiv:0906.2219 [hep-ex]].
7. J. P. Lees *et al.* [BaBar Collaboration], Phys. Rev. D **88** (2013) 071102 [arXiv:1210.5669 [hep-ex]].
8. P. del Amo Sanchez *et al.* [BaBar Collaboration], Phys. Rev. Lett. **107** (2011) 021804 [arXiv:1007.4646 [hep-ex]].
9. J. P. Lees *et al.* [BaBar Collaboration], Phys. Rev. Lett. **107** (2011) 221803 [arXiv:1108.3549 [hep-ex]].
10. J. P. Lees *et al.* [BaBar Collaboration], Phys. Rev. D **88** (2013) 3, 031701 [arXiv:1307.5306 [hep-ex]].
11. B. Aubert *et al.* [BaBar Collaboration], Nucl. Instrum. Meth. A **479** (2002) 1 [hep-ex/0105044].
12. B. Aubert *et al.* [BaBar Collaboration], Nucl. Instrum. Meth. A **729** (2013) 615 [arXiv:1305.3560 [physics.ins-det]].

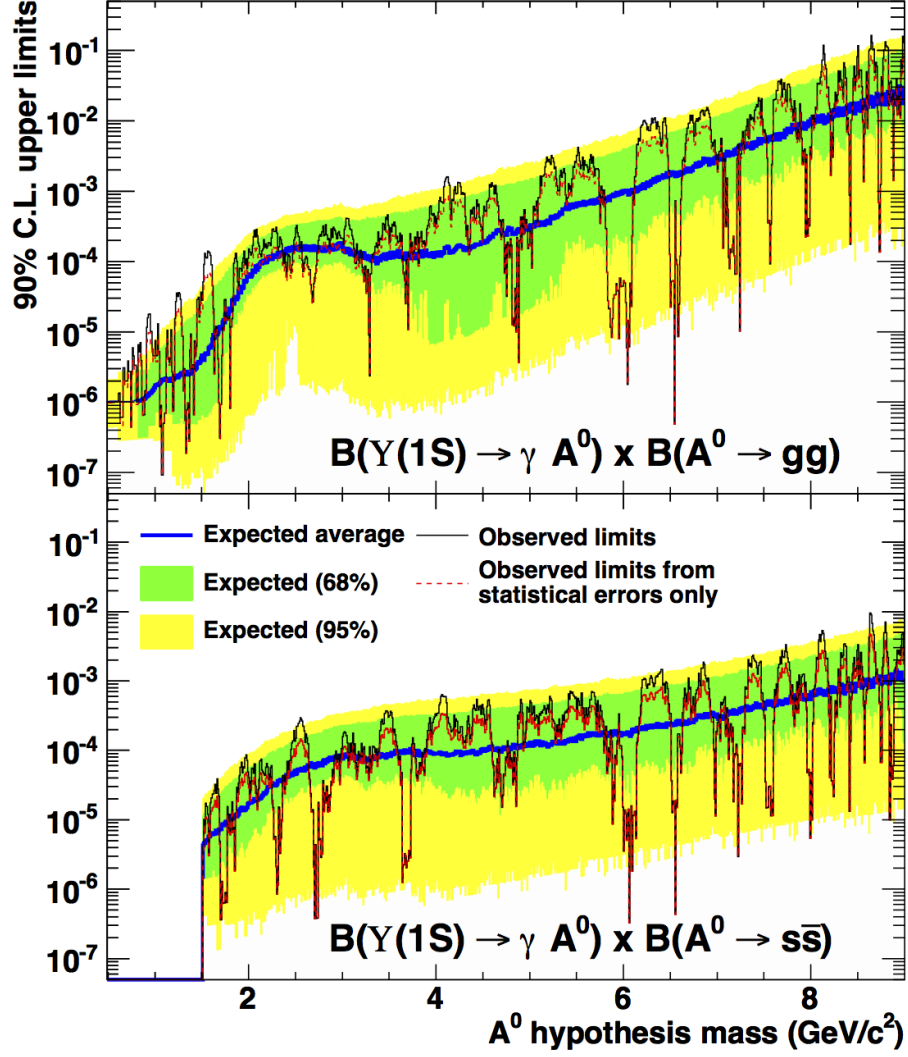


Figure 2: The 90% confidence level upper limits (thin solid line) on the product branching fractions  $\mathcal{B}(Y(1S) \rightarrow \gamma A^0) \times \mathcal{B}(A^0 \rightarrow gg)$  (top) and  $\mathcal{B}(Y(1S) \rightarrow \gamma A^0) \times \mathcal{B}(A^0 \rightarrow s\bar{s})$  (bottom). We overlay limits calculated using statistical uncertainties only (thin dashed line). The inner band is the expected region of upper limits in 68% of simulated experiments. The inner band plus the outer band is the expected region of upper limits in 95% of simulated experiments. The bands are calculated using all uncertainties. The thick line in the center of the inner band is the expected upper limits calculated using simulated experiments.